# Collision-Induced Dissociation and Theoretical Studies of $Ag^+(methanol)_n$, $n = 1-4$

**Hideya Koizumi, Melissa Larsen, and P. B. Armentrout***

*Department of Chemistry, University of Utah, Salt Lake City, Utah 84112*

**David Feller***

*Chemical Sciences Division, Environmental Molecular Sciences Laboratory, Pacific Northwest National Laboratory, MS K1-83, P.O. Box 999, Richland, Washington 99352*

*Received: October 17, 2002; In Final Form: February 14, 2003*

Collision-induced dissociations of the $Ag^+(methanol)_n$ complexes for $n = 1-4$ are studied using kinetic energy dependent guided ion beam tandem mass spectrometry. In all cases, the primary products are endothermic loss of an intact neutral ligand from the complex. The cross section thresholds are interpreted to yield 0 and 298 K bond dissociation energies (BDEs) after accounting for the effects of multiple ion−molecule collisions, internal energy of the complexes, and unimolecular decay rates. These values are compared with theoretical values obtained using high-level ab initio calculations. Generally, good agreement is found except for the third ligand. The nature of the bonding in these complexes and their BDEs are examined in detail. Although the effect is not as dramatic as in singly or doubly ligated copper complexes, 5s−4d$\sigma$ hybridization found in the $Ag^+(methanol)_n$ complexes, $n = 1$ and 2, enhances the BDEs.

## I. Introduction

Noncovalent interactions play a significant role in molecular recognition. Such interactions involve a subtle interplay of entropic and enthalpic effects that are difficult to separate. Theoretical and experimental gas-phase data on such systems are one means of elucidating these effects and providing fundamental insight into the basis of molecular recognition. Our studies are motivated by an interest in developing the principals of molecular recognition for use in advanced chemical separations[1] and analytical methodology.[2] Previously, sequential noncovalent interactions between alkali metal ions[3−8] ($Li^+$, $Na^+$, $K^+$, $Rb^+$, and $Cs^+$) as well as copper and silver ions[9,10−12] and up to four neutral monodentate ligands such as water and dimethyl ether (DME) as well as multidentate ligands[4−7,13] such as dimethoxyethane (DXE) and crown ethers have been examined experimentally by using guided ion beam tandem mass spectrometry. As part of a related ongoing effort to characterize the theoretical requirements for treating such systems, a variety of cation/ligand complexes have been examined with ab initio electronic structure methods. In each case, the complex was composed of a single metal cation, $M^+$, and up to nine oxygen bearing ligands that include the ligands studied experimentally. These cations included the alkali metals ($Li^+$, $Na^+$, $K^+$, $Rb^+$, and $Cs^+$)[3,14−17] and alkaline earths ($Mg^{2+}$, $Ca^{2+}$, $Sr^{2+}$, $Ba^{2+}$, and $Ra^{2+}$),[18] as well as the three coinage metals ($Cu^+$, $Ag^+$, and $Au^+$).[19,20]

For those cases for which reliable experimental data were available, the overall level of agreement between theory and experiment for incremental binding energies was moderate to good. The lack of uniformity in the level of agreement persisted despite the use of a high-level theoretical treatment that in a different regime demonstrated the capability of predicting covalent binding energies to within 4−8 kJ/mol.[21−32] Because quantities such as the dissociation energy of diatomic molecules are known to converge much more slowly with the basis set and level of theory than the electrostatic interactions present in metal/ligand complexes, it is plausible to expect theoretical techniques that perform well in the former case to work well for $M^+(L)_n$ complexes. For those complexes where agreement between theory and experiment was poor, no clear picture emerged as to its cause. As an example of the typical level of agreement between theory and experiment, binding energies for the $Ag^+(H_2O)_n$ complexes are 134 (theory) vs 139 ± 9 (expt); 117.2 (theory) vs 106 ± 1 (expt); 52 (theory) vs 63 ± 1 (expt), and 56 (theory) vs 62 ± 1 (expt) kJ/mol in the order $n = 1$ to 4.[12,20] Yet another example comes from work on the $Cu^+(DME)_n$ complexes, where binding energies are 203 (theory) vs 185 ± 12 (expt); 212 (theory) vs 193 ± 8 (expt); 58 (theory) vs 55 ± 4 (expt) and 48 (theory) vs 45 ± 10 (expt) kJ/mol for $n = 1-4$.[10,19] In general, progress in resolving the discrepancies between theory and experiment is hampered by the difficulty of analyzing the experimental data and the overall scarcity of high-quality experimental measurements and corresponding high-level theoretical predictions.

In this project, we investigate the binding of $Ag^+$ to 1−4 methanol (MeOH) molecules. Guided ion beam mass spectrometry is used to measure the kinetic energy dependent cross sections for collision-induced dissociation (CID). Analysis of these results provides absolute binding energies of these complexes after consideration of reactant energy distributions, effects of multiple collisions, and lifetime effects. These results are compared to high-level ab initio theoretical results.

## II. Experimental and Theoretical Methods

**A. Experimental Approach.** For all reactions studied here, cross sections are collected using a guided ion beam tandem mass spectrometer described previously.[33−35] $Ag^+(MeOH)_n$ complexes are produced in a dc discharge flow tube ion source. At the front end of a meter long flow tube, a dc discharge in a ~10% mixture of Ar in He creates $Ar^+$ ions that sputter metal ions from a silver cathode. The overall pressure is about 0.5 Torr and typical operating conditions of the dc discharge are

10.1021/jp0222548 CCC: $25.00 
Published on Web 04/01/2003

**TABLE 1: Basis Set Combinations and Cation Energies in Hartrees[a]**

| label | Ag | $E_{MP2}(Ag^+,{}^1S)$ | $E_{CCSD(T)}(Ag^+,{}^1S)$ | H,C,O |
|---|---|---|---|---|
| 6-31+G*/RECP | [6s,5p,3d,1f] | −146.18688 | −146.18238 | 6-31+G* |
| aVDZ/RECP | [6s,5p,3d,1f] | −146.18688 | −146.18238 | aug-cc-pVDZ |
| aVTZ/RECP | [8s,7p,5d,2f,1 g] | −146.50624 | −146.49715 | aug-cc-pVTZ |
| aVQZ/RECP | [10s,9p,7d,4f,2 g,1h] | −146.64905 | | aug-cc-pVQZ |

[a] The relativistic effective core potential for silver has a $28e^-$ (Ar + $3d^{10}$) core. There are 18 active electrons.

1.3 kV and 20 mA. Methanol molecules are introduced about 50 cm downstream of the source and attached to the silver ions by three-body condensation. While the complexes traverse the remainder of the flow tube, they are thermalized by undergoing $>10^4$ collisions with the bath gases. The assumption of efficient thermalization is reasonable, as suggested by previous work.[9,36−38]

The ions are extracted from the source, accelerated, and focused into a magnetic sector momentum analyzer for mass analysis. The mass-selected ions are slowed to a desired kinetic energy and focused into a radio frequency (rf) octopole ion guide.[35,39] The guide passes through a static gas cell containing xenon gas, used in our CID studies for reasons described elsewhere.[9,40] After exiting the gas cell, product and remaining reactant ions drift to the end of the octopole, where they are extracted and focused into a quadrupole mass filter for mass analysis. A secondary electron scintillation ion counter detects the mass-analyzed reactant and product ions. These signals are converted to absolute reaction cross sections as described previously.[33] Absolute uncertainties in these cross sections are estimated to be ±20%.

Sharp features in observed cross sections are broadened by thermal motion of the xenon gas and the distribution of ion energies (kinetic and internal). The distribution and absolute zero of the ion kinetic energies are measured using the octopole as a retarding potential analyzer.[33] The uncertainty in the absolute energy scale is ±0.05 eV (lab). Typical distributions have a full width at half-maximum (fwhm) around 0.3 eV (lab). Kinetic energies in the laboratory frame are converted to ion energies in the center-of-mass (CM) frame by $E(\mathrm{CM}) = E(\mathrm{lab})m/(M + m)$, where $M$ and $m$ are ion and neutral reactant masses, respectively. All energies cited in this paper are in the CM frame except as noted.

**B. Theoretical Methods.** Electronic structure calculations provide no direct formal error bars that can be used as a guide to their accuracy. Consequently, to demonstrate convergence of the primary 1-particle and *n*-particle expansions, it is necessary to systematically probe the sensitivity of the predicted properties to changes in the underlying basis set and level of correlation recovery. In the former case, demonstrating convergence translates into carrying out a series of calculations with basis sets that ultimately lead to the complete basis set (CBS) limit. To accomplish this in the context of the present work, basis sets for H, C, and O were taken from the diffuse function augmented correlation consistent basis sets, aug-cc-pVnZ, n = D, T, Q, and 5.[41,42] A "small core" relativistic effective core potential (RECP), taken from the work of Andrae et al.,[43] was used for silver. It replaces a $28e^-$ core (Ar+$3d^{10}$), leaving 18 electrons ($4s^24p^65s^24d^8$) to be handled explicitly. It is labeled ECP28MWB in the Stuttgart ECP naming convention. Because correlation consistent transition metal basis sets have not been reported, we adopt the Ag RECP basis sets developed for our studies of $M^+(H_2O)_n$ and $M^+$(dimethyl ether)$_n$ complexes.[19,20] The composition of the Ag basis sets and the pairing of metal and nonmetal basis sets is given in Table 1, along with the second-order Møller−Plesset (MP2) and coupled cluster with singles, doubles, and perturbative triples excitation (CCSD(T)) energies. A shortened notation (e.g., aVDZ), is used to denote a particular combination of metal and nonmetal basis sets. In addition to the correlation consistent basis sets, for the largest of the methanol (MeOH) complexes, $Ag^+(MeOH)_4$, it was necessary to use the smaller 6-31+G* basis set[44−46] when computing the vibrational normal modes to avoid excessive computational cost.

Unless otherwise noted, all calculations were performed within the frozen core approximation in which the carbon and oxygen 1s electrons were excluded from the correlation treatment. Core/valence (CV) corrections to the binding energies were obtained from all electron MP2 calculations using the correlation consistent cc-pCVTZ basis sets.[47] Experience with even larger core/valence basis sets suggests that obtaining the CV correction at this level of theory should be accurate to ±1 kJ/mol or better.

Most geometries were optimized to the equivalent of the "tight" criterion in Gaussian, i.e., a maximum gradient component of $1.5 \times 10^{-5}$ hartree ($E_h$). Because of the time-consuming nature of these calculations, only the aVDZ basis set was used in optimizing the geometry for complexes involving more than one methanol ligand.

Only the spherical component subset (e.g., 5-term d functions, 7-term f functions, etc.) of the Cartesian polarization functions were used. Calculations were performed with Gaussian 98,[48] MOLPRO-2000,[49] and NWChem.[50] The last application ran in parallel on the Molecular Science Computing Facility's 512-node IBM SP. The largest MP2 calculation in the current study involved 1505 basis functions and required approximately 2 days to complete on 256 processors.

The use of large, diffuse function augmented basis sets such as the aVQZ set can cause linear dependency problems resulting from the presence of multiple ligands in the same small region of space around the metal cation. In particular, severe cases, it may be impossible to converge the Hartree−Fock calculations if nothing is done to minimize the problem. Therefore, in the present work, a threshold of $10^{-5}$ on the eigenvalues of the overlap matrix was selected for the elimination of near linearly dependent basis functions. In practice, this threshold resulted in a maximum of 13 vectors being eliminated in the case of $Ag^+(MeOH)_4$. Although the removal of eigenvectors from the basis function space in this manner can increase the total energy by several tenths of a millihartree, the effect on energy *differences* should be significantly smaller because the same threshold was used on the complex and its constituent fragments.

## III. Results

**A. Experimental Observations; CID of $Ag^+(MeOH)_n$.** Experimental cross sections for the collision-induced dissociation (CID) of $Ag^+(MeOH)_n$, $n = 1-4$, complexes with xenon are shown in Figure 1. In all cases, the dominant process observed for all four complexes is the loss of a single MeOH ligand in reaction 1. For $n = 1$, the primary $Ag^+$ ion product

$$Ag^+(MeOH)_n + Xe \rightarrow Ag^+(MeOH)_{n-1} + MeOH + Xe \quad (1)$$

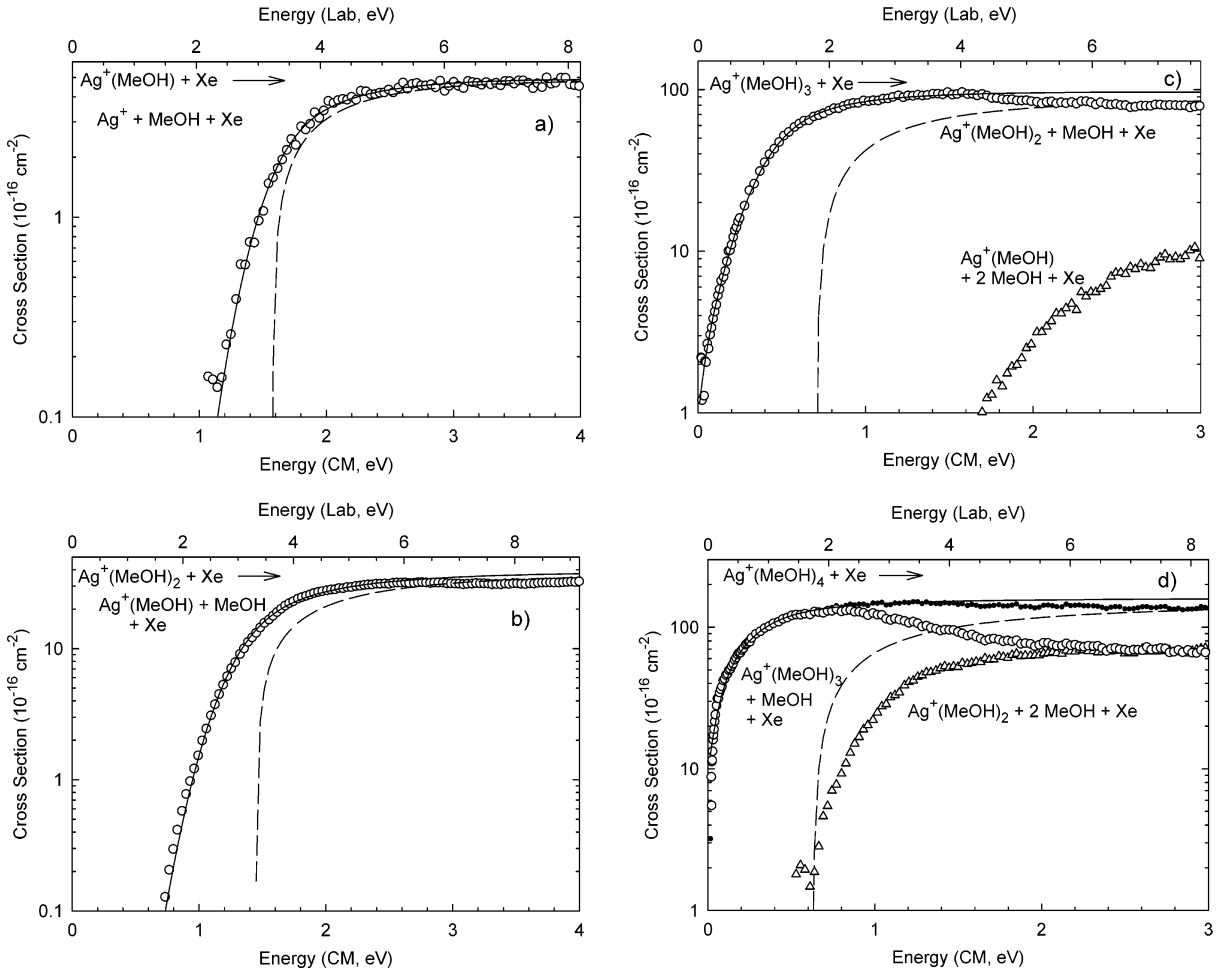


**Figure 1.** Cross sections for reactions of $Ag^+(MeOH)_n$, $n = 1-4$ (parts a−d, respectively), with xenon as a function of kinetic energy in the center-of-mass frame (lower *x* axis) and laboratory frame (upper *x* axis). The dashed lines show the model of eq 2 for the reactants with no internal energy and in the absence of kinetic energy broadening. Solid lines are this model convoluted with the internal and kinetic energy distributions of the reactants. In part d, the solid circles show the total experimental cross section.

cross section has an apparent threshold near 1 eV and levels off with a maximum magnitude near 5 Å$^2$. For $n = 2$, the primary $Ag^+(MeOH)$ ion product cross section has an apparent threshold near 0.7 eV and levels off with a maximum magnitude of 32 Å$^2$. For $n = 3$ and 4, the $Ag^+(MeOH)_{n-1}$ primary product ion cross sections have apparent thresholds near 0 eV. Also, small amounts of $Ag^+(MeOH)_{n-2}$ secondary products are observed at higher energies, clearly the result of sequential dissociation of two MeOH ligands. No other products were observed at any energies, including ligand exchange processes leading to $Ag^+(MeOH)_{n-1}(Xe)$ products.

**B. Thermochemical and Threshold Analysis.** The kinetic energy dependence of the experimental cross sections is modeled using eq 2, where $E$ is the relative translational energy of the

$$\sigma(E) = \sigma_0 \sum g_i(E + E_i - E_0)^N/E \qquad (2)$$

reactants, $E_0$ is the 0 K threshold of the reaction, $\sigma_0$ is an energy-independent scaling factor, and $N$ is an adjustable parameter. The sum is over the rovibrational states of the reactant ion, having energies $E_i$ and populations $g_i$ (where $\Sigma g_i = 1$). The vibrational frequencies of the complexes are taken from the ab initio calculations described below. The Beyer−Swinehart algorithm[51,52] is used to calculate the distribution of internal states of the complex at 300 K, the temperature of the gas in the flow tube.

To analyze the kinetic energy dependence of these cross sections and acquire accurate thermochemistry, several effects have to be considered. First, the internal energy of the reactants must be well-characterized. This is achieved by use of the flow tube ion source, yielding internal energy distributions that should be Maxwellian. Second, the collision gas must provide efficient kinetic to internal energy transfer. Using Xe gas satisfies this condition[9,40] because it is heavy, polarizable, and has no internal modes to carry away energy. Third, rigorous single collision conditions are required to avoid problems associated with depositing excess (and unknown) energy in secondary collisions. To produce rigorous single-collision conditions, data obtained at different neutral reactant pressures (∼0.05, 0.1, 0.2 mTorr) are extrapolated to zero pressure by linear regression.[53] These are the cross sections shown in Figure 1.

Fourth, because the ions move through the apparatus in a finite time (∼0.5 ms), it is important to consider the lifetime of dissociating ions, particularly for large complexes such as $Ag^+(MeOH)_3$ and $Ag^+(MeOH)_4$. The lifetime effect is taken into account using the Rice−Ramsperger−Kassel−Marcus (RRKM) theory[52,54] in the phase space limit (PSL) using equations developed by Rodgers, Ervin, and Armentrout.[55] Briefly, the transition state (TS) for dissociation is modeled by loosely interacting products such that both fragments are free to rotate. This PSL is appropriate for ion−molecule complexes because the TS for the reverse, barrierless association process is accurately described as lying at the top of the centrifugal barrier. In this study, the 2-D external rotations are treated adiabatically but with centrifugal effects included, consistent with the

**TABLE 2: Parameters of Equation 2 Used to Model Data[a]**

| reactant ion | $s_0$ | $N$ | $E_0$ (no RRKM) (eV) | $E_0$ (PSL) (eV) | $\Delta S^{\ddagger}_{1000}$ [J/(K mol)] |
|---|---|---|---|---|---|
| $Ag^+(MeOH)$ | 10.8 (0.5) | 0.6 (0.2) | 1.58 (0.08) | 1.58 (0.08) | 14 (7) |
| $Ag^+(MeOH)_2$ | 67.2 (2.4) | 0.8 (0.2) | 1.46 (0.08) | 1.43 (0.07) | 38 (13) |
| $Ag^+(MeOH)_3$ | 122.1 (7.6) | 0.9 (0.2) | 0.73 (0.06) | 0.69 (0.06) | 37 (13) |
| $Ag^+(MeOH)_4$ | 171.9 (5.8) | 1.0 (0.2) | 0.66 (0.07) | 0.58 (0.08) | 50 (13) |

[a] Uncertanties are listed in parentheses.

discussion of Waage and Rabinovitch.[56] The adiabatic 2-D rotational energy is treated using a statistical distribution with explicit summation over the possible values of the rotational quantum number, as described in detail elsewhere.[55] The model in which the adiabatic 2-D rotational energy is treated using a statistical distribution with average rotational energy gave nearly identical results (much less than 0.01 eV difference). Of course, alternate assumptions about the appropriate transition state for dissociation could be made, but as the PSL TS is the loosest possible transition state, such assumptions would uniformly increase the kinetic shift, thereby decreasing the threshold energies measured in all cases. Previous work finds little justification for such tighter transition states in metal−ligand systems such as those studied here.[55]

Because the rotational, vibrational, and translational energy distributions are explicitly included in our modeling, the threshold energies determined with eq 2 correspond to 0 K. By assuming that $E_0$ represents the energy difference between the reactants and products at 0 K,[57] threshold energies for CID reactions are equated with 0 K bond dissociation energies (BDEs). This correspondence is generally true for ion−molecule reactions because the presence of activation barriers in excess of the reaction endothermicity is unlikely,[58,59] especially for the simple heterolytic bond cleavages considered here.[60] The reported thresholds for all reactions are determined in the following way. First, eq 2 with an initial set of parameters is convoluted with the kinetic energy distribution of the ion beam and the thermal motion of Xe gas in the reaction cell. The parameters of eq 2 are optimized using a nonlinear least-squares analysis to give a best fit to the zero pressure extrapolated cross sections. This represents the threshold energy at 0 K without lifetime corrections. The threshold energies including the PSL analysis provide the bond energy at 0 K including lifetime corrections. An estimate of the uncertainty in the threshold energy is obtained by variations in the parameter $N$ in eq 2, variations in the time available for reaction by factors of 2 and $^1/_2$, variations associated with uncertainties in the vibrational frequencies (±10% for most modes and ± a factor of 2 for metal−ligand modes), and the error in the absolute energy scale (±0.05 eV lab). Threshold energies along with the optimum fitting parameters, $\sigma_0$ and $N$, are listed in Table 2.

Table 2 also includes values for the entropies of activation, $\Delta S^{\dagger}$, a measure of the tightness or looseness of the TS. These values are calculated at 1000 K using molecular parameters calculated below, a rigid-rotor/harmonic oscillator approximation, and standard thermodynamic formulas. The $\Delta S^{\dagger}$(PSL) values can be seen to increase as the number of ligands increases and can be favorably compared to $\Delta S^{\dagger}_{1000}$ values in the range of 29−46 J/(K mol) collected by Lifshitz for several simple bond cleavage dissociations of ions.[61] Considering that the TS is expected to lie at the centrifugal barrier for association of $Ag^+(MeOH)_{n-1}$ + MeOH, the large positive entropies of activation are reasonable.

**C. Theoretical Geometries of $Ag^+(MeOH)_n$ Complexes.** MP2 optimized structures of the $Ag^+(MeOH)_n$ complexes are displayed in Figure 2. Table 3 lists some additional geometrical parameters discussed below. Although methanol possesses $C_s$ symmetry, the $Ag^+(MeOH)$ (1+0) complex lacks even a plane of symmetry. The notation ($m$+$n$) indicates that there are "$m$" methanol molecules in the first solvation shell (i.e., directly bonded to the silver cation) and "$n$" molecules in the second solvation shell (i.e., hydrogen bonded to methanols in the first solvation shell). The $H_aCOAg$ dihedral angle (see Figure 2), which would be zero if the complex were to have $C_s$ symmetry, has values in the range of 16−28° depending on the size of the basis set used. Because the rotational potential around the $Ag^+$−O electrostatic bond is very shallow, it is possible that large basis set CCSD(T) optimization with a tight convergence criterion would find a $C_s$ symmetry minimum, but CCSD(T) optimizations with the aug-cc-pVDZ and aug-cc-pVTZ basis sets give no hint of this. The $Ag^+$−O distance is seen to be moderately sensitive to the choice of basis set, decreasing by 0.026 Å as the size of the basis set is increased from aVDZ to aVQZ. Compared to the $Ag^+$−O distance in the $Ag^+(H_2O)$ complex,[20] the value in $Ag^+(MeOH)$ is 0.026 Å shorter at the MP2/aug-cc-pVQZ level, reflecting a moderate increase in the bond strength. Likewise, the $r_{MO}$ distance in the $Ag^+$(DME) complex[19] is shorter than the corresponding distance in $Ag^+$-(MeOH) by 0.016 Å at the MP2/aug-cc-pVQZ level. At the CCSD(T) level of theory the $Ag^+$−O distance lengthens by 0.017 Å, but the potential is quite soft. Bond lengths in the methanol fragment change by no more than 0.003 Å and bond angles by no more than 2°. On the basis of this level of agreement, we conclude that MP2 is probably capable of yielding accurate geometries for the larger complexes where CCSD(T) optimizations are prohibitively expensive.

**TABLE 3: Selected Geometrical Parameters of the Lowest Energy MP2 Optimized Structures of the $Ag^+(MeOH)_n$ Complexes[a]**

| species | $Ag^+$−O (Å) | ∠O$Ag^+$O (deg) | ∠$Ag^+$OH (deg) | ∠$Ag^+$OC (deg) |
|---|---|---|---|---|
| $Ag^+(MeOH)$ (1+0) | 2.165 | | 121.6 | 126.7 |
| $Ag^+(MeOH)_2$ (2+0) | 2.124 | 175.6 | 119.3 | 122.6 |
| | 2.124 | | 119.3 | 122.6 |
| $Ag^+(MeOH)_3$ (3+0) | 2.183 | 139.0 | 119.5 | 123.4 |
| | 2.264 | 85.3 | 122.6 | 120.6 |
| | 2.273 | | 123.7 | 120.2 |
| $Ag^+(MeOH)_4$ (4+0) | 2.371 | 86.7 | 127.7 | 121.0 |
| | 2.241 | 150.1 | 120.5 | 117.6 |
| | 2.254 | 76.1 | 106.8 | 129.0 |
| | 2.392 | | 124.1 | 112.8 |

[a] MP2/aug-cc-pVDZ level of theory.

When a complex contains two or more MeOH ligands, there is a competition between $M^+$−O bonding and hydrogen bonding between ligands. As shown in Figure 3, the hydrogen bond between two methanol molecules calculated at the MP2 complete basis set limit falls near 24 kJ/mol, which compares to 21 kJ/mol for the water−water hydrogen bond.[62] In accord with this increase in bond strength, the O−O distance in $(MeOH)_2$ is 0.064 Å shorter than the corresponding distance in $(H_2O)_2$. Similarly, the O−H distance between the proton being donated and the oxygen of the second MeOH is 1.887 Å, compared to 1.951 Å in the water dimer.

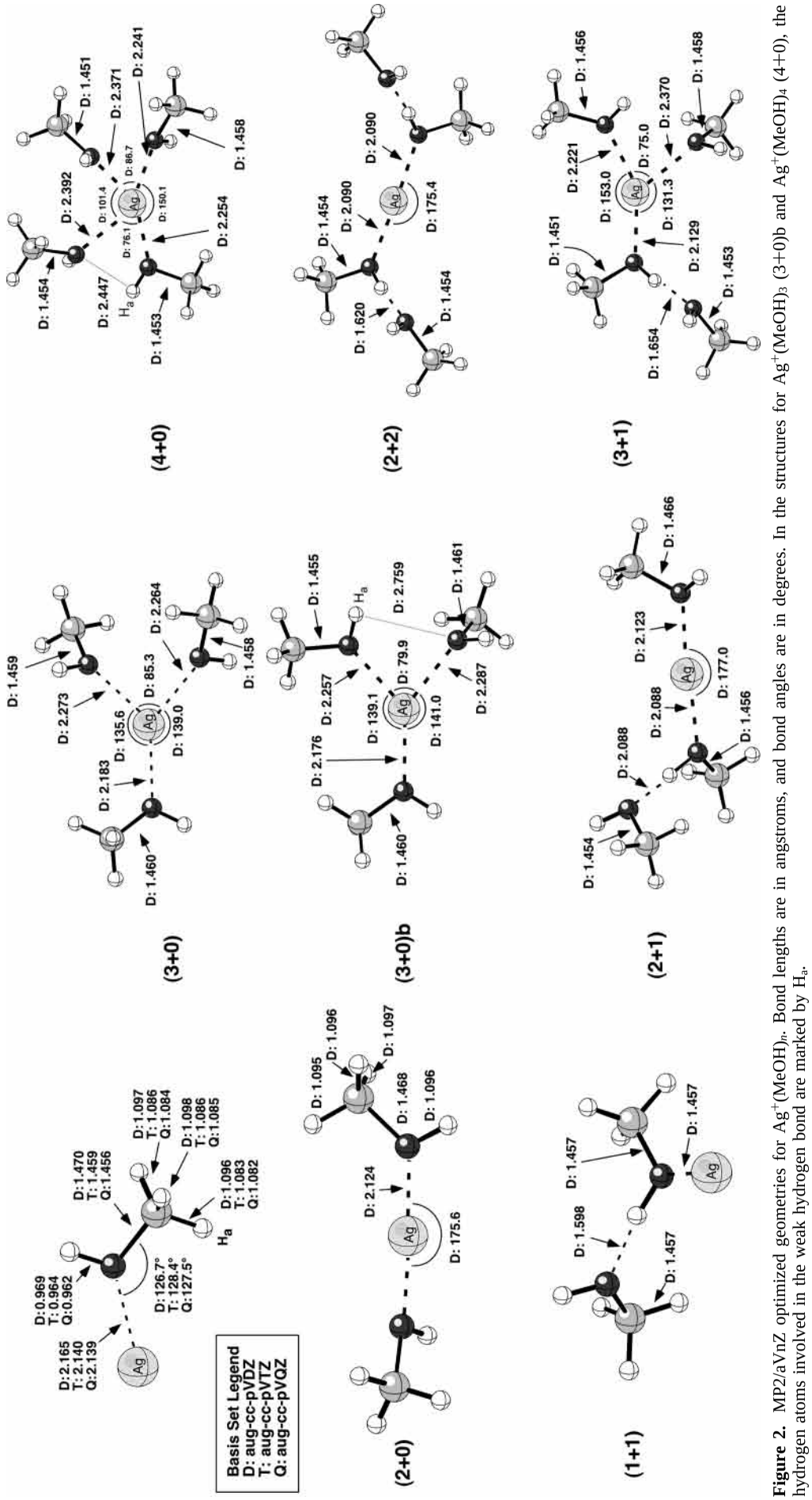


**Figure 2.** MP2/aVnZ optimized geometries for $Ag^+(MeOH)_n$. Bond lengths are in angstroms, and bond angles are in degrees. In the structures for $Ag^+(MeOH)_3$ (3+0)b and $Ag^+(MeOH)_4$ (4+0), the hydrogen atoms involved in the weak hydrogen bond are marked by $H_a$.

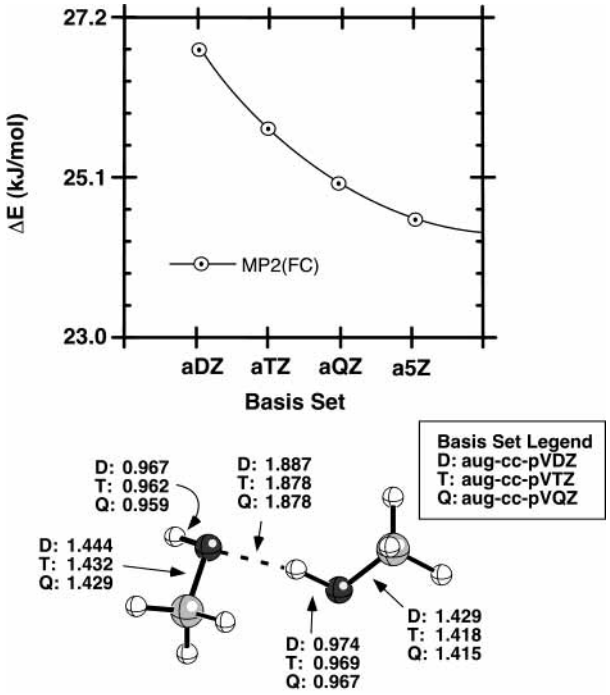


**Figure 3.** MP2 convergence of the electronic (vibrationless) binding energy of the methanol dimer as a function of the basis set size. MP2/aVnZ optimized geometries for the methanol dimer. Bond lengths are in angstroms and bond angles are in degrees.

In the $Ag^+(MeOH)_2$ (2+0) complex, the O−$Ag^+$−O bond angle is 175.6° at the MP2/aVDZ level of theory, nearly identical to the 177.3° in $Ag^+(DME)_2$ and close to the 180° in $Ag^+(H_2O)_2$.[19,20] For both $n = 1$ and 2, the $Ag^+$−O−C bond angles are larger than $Ag^+$−O−H (Table 3) because the complexes try to minimize the repulsive interaction between the methyl groups and the $Ag^+$ cation. The dihedral angle formed between the two C−O−H planes is 70.8°, as this puts the p-like oxygen lone pairs into nearly perpendicular planes such that the ligand−ligand repulsive interaction is minimized. The dihedral angle between the two C−O bonds is 115.8°, presumably larger than 90° because the methyl groups are more repulsive with one another than with the smaller H atoms. A second structure, lying 3.8 kJ/mol higher in energy, was identified. As seen in Figure 2, it possesses a (1+1) topology.

With three ligands, the lowest lying (3+0) complex adopts a distorted Y conformation (see Figure 2), with two long $Ag^+$−O bonds (2.273 and 2.264 Å) and one short (2.183 Å). The methanol ligands at long distances form an acute angle of 85.3° with the central metal. As for the $n = 1$ and 2 complexes, the bond angle formed by $Ag^+$−O−H is smaller than $Ag^+$−O-C for the tightly bound MeOH ligand, whereas the opposite is true for the two loosely bound MeOH ligands. Presumably, this difference is a result of minimizing the repulsive interaction between these two ligands, while keeping the $Ag^+$−O bond distances as short as possible. For the two loosely bound MeOHs, the dihedral angle between the two C−O−H planes is 89.0°, which again puts the oxygen lone pairs into perpendicular planes. Here, the dihedral angle is closer to 90° than the one in the bis-ligated complex because of the smaller distance between two MeOH ligands. Angles of 0° and 180° are disfavored by the repulsive interactions between methyl groups and $Ag^+$ and between two methyl groups. The metal cation and methanol oxygens are within 4° of being coplanar.

Two other $Ag^+(MeOH)_3$ structures were examined. One was a second (3+0) conformation, which is obtained from the lower energy (3+0) structure by rotating one of the methanols so that a very weak hydrogen bond can be formed. This structure lies 0.2 kJ/mol higher in energy when zero point vibrational energies are taken into account. No attempt was made to locate additional minima possessing weak hydrogen bonds. The third structure has a (2+1) topology and is 0.4 kJ/mol above the lowest energy conformation. Both the (3+0)b and (2+1) structures were verified to be minima on the $Ag^+(MeOH)_3$ hypersurface by performing normal-mode analyses. A (1+1+1) complex is possible, but judging by the relative energy of the (2+1) complex, it will lie even higher in energy and so will not be pursued.

With four MeOH ligands, the optimized structure for the lowest energy form of $Ag^+(MeOH)_4$ (4+0) possesses $C_1$ symmetry. There are pairs of long and short $Ag^+$−O bonds positioned on either side of the silver ion. The short bond lengths in $Ag^+(MeOH)_4$ are comparable in length to the long bonds in $Ag^+(MeOH)_3$, presumably because of the much larger ligand−ligand repulsion. One pair of bonds has an O−$Ag^+$−O angle 86.7° and bond lengths of 2.241 and 2.371 Å, whereas the other pair has an angle of 76.1° and bond lengths of 2.254 and 2.392 Å. The O−$Ag^+$−O angle formed by the two short $Ag^+$−O bonds is 150.1°, much larger than 109.7° found in tetrahedral structures, whereas the two long bonds have an angle of 101.4°, close to the tetrahedral angle. The dihedral angle between the two C−O−H planes of the two methanol ligands that are associated with the 86.7° O−$Ag^+$−O bond angle is 86.7°, similar to the dihedral angle found between the comparable ligands in the $Ag^+(MeOH)_3$ complex. In contrast, this dihedral angle is 61.8° for the pair of ligands having the 76.1° O−$Ag^+$−O bond angle, which we believe may be a consequence of a weak hydrogen bond between these two ligands. Further evidence for this comes from analyzing the $Ag^+$−O−H bond angles compared to the $Ag^+$−O-C bond angles (Table 3). For the MeOHs having a 86.7° O−$Ag^+$−O angle, the $Ag^+$−O−H bond angles are larger than the $Ag^+$−O-C bond angles, as also observed for the two loosely bound MeOH ligands in $Ag^+(MeOH)_3$. In the pair of ligands having the 76.1° O−$Ag^+$−O bond angle, this is also true for the loosely bound MeOH ligand, but for the tightly bound ligand ($Ag^+$−O bond length of 2.254 Å), the $Ag^+$−O−H bond angle is much smaller than the $Ag^+$−O-C bond angle. The $Ag^+$−O−H angle for this MeOH is 17° smaller than the average of the $Ag^+$−O−H angles found in the other three MeOH ligands. The hydrogen atom ($H_a$) of the OH group in this MeOH ligand has a fairly short distance to the oxygen atom of the adjacent ligand (2.447 Å vs 1.951 Å in the water dimer), creating the acute O−$Ag^+$−O angle of 76.1°. This partial hydrogen bond, which judging by the proton−oxygen distance is slightly stronger than the weak hydrogen bond in the $Ag^+(MeOH)_3$ (3+0)b structure, leads to the distortions in the structure observed and bears some similarity to the lowest energy conformation of $Ag^+(H_2O)_4$ which has a (3+1) topology.[20] The fourth water forms simultaneous hydrogen bonds to two waters in the first solvation shell. This permits a shorter average $M^+$−O distance than is found in $Ag^+(MeOH)_4$, 2.25 vs 2.32 Å. Because the DME ligand cannot engage in hydrogen bonding, $Ag^+(DME)_4$ adopts an $S_4$ high-symmetry conformation with uniform $M^+$−O distances of 2.28 Å.

Conformations with (2+2) and (3+1) topologies were also located on the $Ag^+(MeOH)_4$ hypersurface. Both structures were 0.4 kJ/mol higher than the (4+0) structure, including zero point energies. The oxygens directly attached to the silver cation are nearly coplanar with the metal.

**TABLE 4: MP2 Normal-Mode Frequencies ($cm^{-1}$)[a]**

| system | frequencies |
|---|---|
| (MeOH) | 311.2, 1044.1, 1074.8, 1169.1, 1366.3, 1465.0, 1493.6, 1505.1, 3053.1, 3130.6, 3189.9, 3841.5 |
| $Ag^+(MeOH)$ | 62.6, 151.6, 323.9, 349.5, 978.3, 1101.9, 1167.1, 1374.9, 1471.4, 1486.1, 1503.9, 3105.5, 3220.9, 3234.9, 3808.4 |
| $Ag^+(MeOH)_2$ | 23.1, 50.6, 57.1, 96.4, 108.5, 161.4, 168.5, 311.3, 374.7, 401.7, 411.8, 982.2, 983.8, 1098.4, 1099.2, 1169.8, 1169.9, 1371.1, 1371.6, 1469.2, 1469.7, 1488.5, 1488.6, 1502.7, 1502.9, 3103.6, 3103.6, 3216.3, 3216.3, 3235.8, 3235.8, 3807.9, 3808.5 |
| $Ag^+(MeOH)_3$ | 19.8, 21.4, 46.4, 56.6, 65.1, 73.5, 74.6, 106.4, 115.3, 151.7, 156.7, 167.4, 239.9, 273.9, 315.5, 350.8, 408.9, 416.3, 1013.1, 1015.2, 1019.5, 1112.8, 1114.5, 1127.1, 1197.2, 1198.4, 1198.7, 1396.4, 1398.9, 1406.7, 1517.8, 1519.2, 1522.1, 1548.9, 1552.6, 1558.4, 1560.4, 1561.8, 1563.6, 3131.0, 3131.3, 3136.6, 3231.5, 3232.0, 3241.9, 3262.3, 3263.0, 3265.1, 3747.6, 3748.5, 3751.9 |
| $Ag^+(MeOH)_4$ | 15.8, 22.5, 28.9, 40.7, 48.1, 54.1, 62.4, 66.2, 88.7, 98.7, 115.6, 126.9, 133.8, 138.3, 146.3, 158.9, 213.9, 226.0, 261.2, 293.2, 382.4, 421.3, 453.6, 530.1, 1017.9, 1021.6, 1030.0, 1036.5, 1102.1, 1107.2, 1112.7, 1113.9, 1198.5, 1199.0, 1199.7, 1201.1, 1377.1, 1393.6, 1395.4, 1398.2, 1517.4, 1520.0, 1520.7, 1521.1, 1552.0, 1552.8, 1553.5, 1558.9, 1560.7, 1562.3, 1563.7, 1566.9, 3122.5, 3123.5, 3127.2, 3128.2, 3218.1, 3221.9, 3225.1, 3226.8, 3248.7, 3250.7, 3257.5, 3263.2, 3729.5, 3738.2, 3747.7, 3747.9 |

[a] Values for MeOH, $Ag^+(MeOH)$, $Ag^+(MeOH)_2$, and $Ag^+(MeOH)_3$ were obtained with the aug-cc-pVDZ basis set. The $Ag^+(MeOH)_4$ frequencies were obtained with the 6-31+G* basis set.

**TABLE 5: Total Energies and Electronic (Vibrationless) Binding Energies**

| complex | | basis set | method | $E_{total}$ ($E_h$) | $\Delta E$ (kJ/mol) |
|---|---|---|---|---|---|
| $Ag^+(MeOH)$ | (1+0) | aVDZ | MP2 | −261.665714 | 149.4 |
| | | | CCSD(T) | −261.693884 | 146.0 |
| | | aVTZ | MP2 | −262.092957 | 151.5 |
| | | | CCSD(T) | −262.114796 | 146.9 |
| | | aVQZ | MP2 | −262.270794 | 154.0 |
| $Ag^+(MeOH)_2$ | (2+0) | aVDZ | MP2 | −377.143793 | 147.3 |
| | | | CCSD(T) | −377.204532 | 143.5 |
| | | aVTZ | MP2 | −377.678682 | 149.0 |
| | | aVQZ | MP2 | −377.891465 | 151.0 |
| | (1+1) | aVDZ | MP2 | −377.118691 | 143.5 |
| $Ag^+(MeOH)_3$ | (3+0) | aVDZ | MP2 | −492.596787 | 81.6 |
| | | | CCSD(T) | −492.690069 | 80.8 |
| | | aVTZ | MP2 | −493.233591 | 68.2 |
| | | aVQZ | MP2 | −493.479070 | 64.4 |
| | (3+0)b | aVDZ | MP2 | −492.595882 | 81.5 |
| | (2+1) | aVDZ | MP2 | −492.594739 | 81.3 |
| $Ag^+(MeOH)_4$ | (4+0) | aVDZ | MP2 | −608.045813 | 71.1 |
| | | aVTZ | MP2 | −608.785498 | 60.2 |
| | | aVQZ | MP2 | −609.063880 | 56.9 |
| | (3+1) | aVDZ | MP2 | −609.044176 | 70.9 |
| | (2+2) | aVDZ | MP2 | −609.044659 | 70.9 |

The limited conformational searching for the $n = 2-4$ complexes that has been performed cannot guarantee that the global minimum has been identified. However, on the basis of our experience with the $Ag^+(H_2O)_n$ and $Ag^+(DME)_n$ systems, we believe it is likely that all relevant low-lying conformations have been considered.

**D. Comparison of Experimental and Theoretical Bond Dissociation Energies.** Calculated harmonic vibrational frequencies are listed in Table 4, and electronic binding energies are given in Table 5. The binding energy of $Ag^+(MeOH)$ is seen to be relatively insensitive to the quality of the basis set or the amount of correlation recovery. Basis set enlargement and increased correlation recovery have opposite effects on the binding energy and are of approximately the same magnitude. Increasing the basis set from aVDZ to aVQZ increases $\Delta E$ by 4.6 kJ/mol, whereas using the higher level CCSD(T) method in place of MP2 decreases $\Delta E$ by 6.3 kJ/mol. As a result, the MP2/aVDZ result lies fortuitously close to the large basis set CCSD(T) limit.

In reporting our binding energies, we have chosen not to correct for the undesirable effects of basis set superposition error (BSSE). Correcting for BSSE would, of necessity, reduce the magnitude of the binding energy even though increasing the size of the basis set monotonically increases $\Delta E$. Thus, a BSSE-corrected value would be farther from the basis set limit than the raw value. Previous experience with cation/ligand complexes found similar behavior.[19,20] For $Ag^+(MeOH)$ the counterpoise correction of Boys and Bernardi predicts a BSSE of 10.5 kJ/mol at the MP2/aug-cc-pVQZ level.[63] For the larger clusters, the BSSE will decrease because the Ag−O distances increase.

**TABLE 6: Experimental and Theoretical Binding Energies (kJ/mol) at 0 K**

| complex | expt $\Delta H_0$ (0 K) | theor $\Delta H_0$ (0 K) | theoretical method |
|---|---|---|---|
| $Ag^+(MeOH)$ | 152 ± 8 | 145.6 | MP2/aVQZ+CCSD(T)+CV |
| $Ag^+(MeOH)_2$ | 138 ± 7 | 140.2 | MP2/aVQZ+CCSD(T)+CV |
| $Ag^+(MeOH)_3$ | 66 ± 6 | 52.3 | MP2/aVQZ+CCSD(T)+CV |
| $Ag^+(MeOH)_4$ | 56 ± 8 | 50.2 | MP2/aVQZ |

Combining the best estimate of the electronic binding energy with the zero point, CCSD(T) and CV corrections leads to a $\Delta H_0$ value of 146 kJ/mol for $Ag^+(MeOH)$. This compares to 132 and 153 kJ/mol for $Ag^+(H_2O)$ and $Ag^+(DME)$, respectively.[19,20]

For $Ag^+(MeOH)_2$, the incremental binding energy, including zero point, CCSD(T), and CV corrections, is 140 kJ/mol (Table 6), representing a small decrease over the binding energy of $Ag^+(MeOH)$. Compared to the corresponding mono-ligated complexes, theoretical calculations predict an increase in BDE for the $Ag^+(DME)_2$ complex, and a decrease for $Ag^+(H_2O)_2$, where the second water is bound by 16 kJ/mol less than the first water. Because a CCSD(T)/aVTZ calculation proved to be prohibitively expensive for $Ag^+(MeOH)_2$, we used the ratio of the aVTZ/aVDZ CCSD(T) corrections from the smaller $Ag^+(MeOH)$ complex to estimate the final bond energy for the bis-ligated complex.

Compared with the $n = 1$ and 2 complexes, the binding energy of the $Ag^+(MeOH)_3$ complex shows greater sensitivity to the size of the basis set, decreasing by 17 kJ/mol over the aVDZ, aVTZ, and aVQZ sequence. The aVQZ value, including zero point, CCSD(T) + CV corrections, is 52 kJ/mol, smaller than the corresponding 58 and 68 kJ/mol values for $Ag^+(H_2O)_3$ and $Ag^+(DME)_3$, respectively.[19,20]

For the tetrakis-ligated complexes, the incremental binding energies follow the order 50 kJ/mol for $Ag^+(MeOH)_4$, 64 kJ/mol for $Ag^+(H_2O)_4$, and 66 kJ/mol for $Ag^+(DME)_4$, which inversely tracks with the average Ag−O bond distance. The incremental binding energy of $Ag^+(MeOH)_4$ is probably slightly too large because it was prohibitively expensive to compute a CCSD(T) adjustment to $\Delta E$, as was done for the other three methanol complexes.

**TABLE 7: Enthalpies and Free Energies for $Ag^+(MeOH)_n$ Dissociation at 0 and 298 K (in kJ/mol)**

| complex | $\Delta H_0$ [a] | $\Delta H_{298} - \Delta H_0$ [b] | $\Delta H_{298}$ | $T\Delta S_{298}$ [b] | $\Delta G_{298}$ |
|---|---|---|---|---|---|
| $Ag^+(MeOH)$ | 152 ± 8 | 1.4 ± 0.2 | 153 ± 7 | 27.2 ± 0.7 | 126.3 ± 1.1 |
| | *145.6* | | *147.0* | | *119.8* |
| $Ag^+(MeOH)_2$ | 138 ± 7 | −0.6 ± 0.3 | 137 ± 6 | 40.3 ± 1.4 | 97.2 ± 1.4 |
| | *140.2* | | *139.6* | | *99.3* |
| $Ag^+(MeOH)_3$ | 66 ± 6 | −1.8 ± 0.3 | 64 ± 4 | 38.4 ± 1.4 | 26.2 ± 2.6 |
| | *52.3* | | *50.5* | | *12.1* |
| $Ag^+(MeOH)_4$ | 56 ± 8 | −1.2 ± 0.3 | 55 ± 10 | 42.2 ± 1.4 | 13.3 ± 1.3 |
| | *50.2* | | *49.0* | | *6.8* |

[a] Values in italics are theoretical values. [b] Calculated using standard formulas and molecular constants determined at the MP2/aug-cc-pVDZ level of theory. The vibrational frequencies of $Ag^+(MeOH)_n$ complexes and MeOH are given in Table 1. Uncertainties correspond to changes in the metal−ligand frequencies by a factor of 2 and ±10% vibrations in the MeOH vibrational frequencies.

The final recommended theoretical BDEs including zero point, CCSD(T), and CV corrections are compared with our experimental values in Table 6. Corrections from 0 to 298 K values are achieved using the information provided in Table 7. Experiment and theory agree that the first and second MeOHs have strong bonds, whereas the third and fourth MeOH ligands bind much more weakly. In semiquantitative agreement with theory, experiment finds that the second BDE is somewhat weaker (by 14 kJ/mol, expt vs 5.4 kJ/mol, theory) than the first. Moreover, the sum of the first and second BDEs are in good agreement (290 kJ/mol, expt vs 286 kJ/mol, theory). Similar trends are observed for the water-ligated silver complexes where the theoretical and experimental sums of first and second BDEs are in good agreement.[12,20]

We note in Table 6 that the level of agreement between theory and experiment is best for the more symmetric complexes ($n = 2$ and 4) and is poorer for the less symmetric systems ($n = 1$ and 3). One possible cause of the deviation between experiment and theory may arise from the inability of the relativistic effective core potential on $Ag^+$ to polarize. This inflexibility would lead to an underestimated BDE for the first ligand, but for two ligands, where the polarization is much more balanced because of the geometry of the $Ag^+(MeOH)_2$ complex, the effect would be nearly absent. The unbalanced situation observed for three ligands could also lead to an underestimated theoretical BDE, whereas the more balanced geometry of the tetrakis-ligated complex would be more accurate. This is consistent with the comparisons with the experimental values for the $Ag^+(MeOH)_n$ complexes. Smaller effects can be imagined for the $Ag^+(H_2O)_n$ complexes because they are bound more loosely than MeOH.

Overall, the experimental values are in reasonable agreement with theoretical values for all values of *n*. The mean absolute deviation between the experimental and ab initio theoretical results are 7 ± 5 kJ/mol for $n = 1-4$ compared to an average experimental uncertainty of 7 kJ/mol. In addition, the sum of the four bond energies is reasonably well predicted: 412 ± 15 kJ/mol (expt) vs 388 (theory).

## IV. Discussion

**A. Effect of d Electrons.** The $Ag^+$ ion has a $^1S$ ($5s^04d^{10}$) ground state electronic configuration. It has been shown that a coinage ion can bind one and two ligands more strongly than an alkali metal ion that has a similar ionic radius as a result of $(n+1)s-nd\sigma$ hybridization. Briefly, as the first ligand approaches a silver metal cation, the doubly occupied $4d\sigma$ orbital hybridizes with the empty 5s orbital. The $5s-4d\sigma$ hybrid localized along the bonding axis is left empty to act as an acceptor orbital for electron density from the ligand. The pair of electrons originally in the $4d\sigma$ orbital occupies the $5s-4d\sigma$ orbital localized perpendicular to the bonding axis. Thus, hybridization reduces the charge density of the metal along the bonding axis, thereby reducing metal−ligand repulsion and increasing the effective nuclear charge seen by the ligand. Because of the symmetry of the $5s-4d\sigma$ hybrid orbitals, a second ligand, located 180° away from the first, can donate electrons to the same empty $5s-4d\sigma$ hybrid orbital. Thus, it also feels less repulsion and a higher nuclear charge, whereas the energetic cost of hybridization is shared by two ligands. Hence, the BDE of the second ligand is much stronger than corresponding BDEs found in analogous alkali metal ion complexes with similar ionic radii. In contrast, the absolute BDEs for $Cu^+(L)_n$ complexes are such that the second ligand binds more strongly than the first. This difference between the two coinage metals is partially explained by the ionic radii, which are 1.26 and 0.96 Å for silver and copper, respectively. The effect of the $(n+1)s-nd\sigma$ hybridization decreases as the ionic radii of the metal ion increases. In addition, the hybridization of $Ag^+$ becomes less effective than that of $Cu^+$ because the d−s excitation energy, which scales with the energy needed to hybridize from the ground state $s^0d^{10}$ configuration to the $s^1d^9$ configuration, is 4.86 eV for $Ag^+$, much higher than that of $Cu^+$ (2.72 eV).[64]

Upon adding further ligands, it is useful to consider the structures of the $n = 3$ and 4 complexes within the context of orbital interactions as usually viewed in organometallic chemistry. The $Ag^+(MeOH)_4$ complex is an 18 $e^-$ species with a $d^{10}$ electronic configuration at the metal. Thus, the complex might be expected to adopt a tetrahedral ligand arrangement, but this is distorted by the hydrogen bonding and ligand−ligand repulsions noted above. For the $Ag^+(MeOH)_3$ complex, a $4d^{10}$ configuration should prefer a trigonal planar geometry (where we will define the molecular plane as the $x-y$ plane).[65] Relative to this trigonal planar geometry, the distortion toward the Y-geometry observed theoretically (Figure 2) increases the energy of the $4d_{xy}$ orbital and stabilizes the $4d_{x^2-y^2}$ orbital. Although both these orbitals are doubly occupied, this is favorable in the present case because the $4d_{x^2-y^2}$ orbital can engage in $5s-4d\sigma$ hybridization and become further stabilized. In essence, the two closely spaced ligands are both donating electrons into the same lobe of the $5s-4d\sigma$ acceptor orbital.

**B. Sequential Binding Energies.** The main attractive forces between the methanol ligand and the silver cation are ion−dipole and ion-induced dipole interactions, which have $r^{-2}$ and $r^{-4}$ dependences, respectively. (The dipole moment and polarizability of MeOH are 1.70 D and 3.25 $Å^3$, respectively.[66]) Therefore, the calculated M−O bond length found in the complex is generally a good measure of how strong the ligand binds to the metal ion. In this study, weaker BDEs are observed as the longest M−O bond found in the complex increases in length. However, as noted above, even though the $Ag^+$−O bond lengths for $Ag^+(MeOH)_2$ are shorter than the bond length in

$Ag^+(MeOH)$, the second MeOH ligand is less strongly bound than the first. (Similarly, theoretical calculations of $Ag^+(H_2O)_n$ complexes find that the first BDE is stronger than the second even though the bond lengths also decrease with increasing ligation.[20]) This trend agrees with the experimental BDEs.

A more quantitative measure of the effect of these electrostatic interactions between $Ag^+$ and the ligand can be determined by calculating the partial charge on the oxygen atom, as determined from a Mulliken population analysis. These partial charges are $-0.24$, $-0.39$, and $-0.65$ for ligands $H_2O$, MeOH, and DME, respectively.[19,20] These values are related to the polarizability of the ligands, 1.45, 3.25, and 5.24 Å$^3$, respectively.[66−68] The $\Delta H_0$ values follow in that same order: 134 ($H_2O$), 154 (MeOH), and 164 (DME) kJ/mol. Of secondary importance is the point charge−dipole interaction, which partially offsets the trend in partial charges, occurring in the order 1.36 (DME), 1.70 (MeOH), and 1.88 ($H_2O$) D.[66−68]

For $n = 3$, the three M−O bond lengths observed here are 2.183, 2.264, and 2.273 Å. Two bonds are longer because the $Ag^+(MeOH)_3$ retains the 5s−4d$\sigma$ hybridization by putting two MeOHs on the opposite side of the MeOH that binds tightly to the $Ag^+$ ion. These two loosely bound MeOHs try to minimize the repulsive interaction between them while keeping the $Ag^+$−O distances as close as possible. The BDE for the third MeOH is significantly weaker than the second because it loses some 5s−4d$\sigma$ hybridization.

For $n = 4$, the geometry deviates from a pseudotetrahedral structure as a result of 5s−4d$\sigma$ hybridization; two tightly bound MeOHs form an O−$Ag^+$−O angle of 150.1°, which is larger than 139.0° found in the $Ag^+(MeOH)_3$ complex where the effect of hybridization is shared by the third MeOH. The fourth MeOH has the longest $Ag^+$−O bond length studied here. However, the BDE of the fourth MeOH is only slightly weaker than the third because the complex still retains most of the 5s−4d$\sigma$ hybridization found in the $Ag^+(MeOH)_3$.

## V. Conclusion

Kinetic energy dependent collision-induced dissociation in a guided ion beam mass spectrometer is used to determine the absolute bond energies of $Ag^+(MeOH)_n$ with $n = 1-4$. Effects of multiple collisions, internal energies of the complexes, reactant translational energy distributions, and dissociation lifetimes are all considered in the analysis of the experiments. Our experimental results as well as theoretical results show strong BDEs for $n = 1$ and 2, decreasing slightly for $n = 2$. These trends in the absolute BDEs differ from those for $Cu^+(L)_n$ complexes where second ligand binds more strongly than the first. The difference is easily rationalized by the increase in ionic radii that reduce the effect of the $(n+1)$s−$n$d$\sigma$ hybridization. Also the hybridization in the $Ag^+$ ion is less effective because the energy needed for d−s promotion is higher.

For $n = 3$, calculations show that the complex tries to retain 5s−4d$\sigma$ hybridization while minimizing the repulsive interaction between two loosely bound MeOH ligands. The resulting BDE for the third MeOH is significantly weaker than the second because hybridization is not as effective as in the $Ag^+(MeOH)_2$ complex and ligand−ligand repulsion is more severe. The BDE of the fourth MeOH is only slightly weaker than the third because it retains the partial 5s−4d$\sigma$ hybridization found in $Ag^+(MeOH)_3$ and ligand−ligand repulsion is comparable. Overall, our experimental BDEs for $Ag^+(MeOH)_n$ complexes are in good agreement with our theoretical results, with the worst agreement occurring for the $(MeOH)_2Ag^+$−MeOH bond energy, which is underestimated by theory.

**Acknowledgment.** This research was supported by the National Science Foundation, CHE-0135517 (P.B.A.), and by the U. S. Department of Energy, Office of Basis Energy Research, Chemical Sciences, under Contract No. DE-AC06-76RLO1830 (D.F.). The participation of M.L. was enabled by support from the NSF REU program, 0097253. This research was performed, in part, using the Molecular Science Computing Facility (MSCF) in the William R. Wiley Environmental Molecular Sciences Laboratory at the Pacific Northwest National Laboratory. The MSCF is a national user facility funded by the Office of Biological and Environmental Research in the U.S. Department of Energy. The Pacific Northwest National Laboratory is a multiprogram national laboratory operated by Battelle Memorial Institute. We thank Dr. David Dixon for a careful reading of this manuscript prior to publication. H. K. thanks Prof. Jay Amicangelo and Prof. M. T. Rodgers for enlightening discussions.

## References and Notes

(1) Horwitz, E. P.; Dietz, M. L.; Fisher, D. E. *Solvent Extr. Ion Exch.* **1991**, *9*, 1.
(2) Grate, J. W.; Strebin, R.; Janata, J.; Egorov, O.; Ruzicka, J. *J. Anal. Chem.* **1996**, *68*, 333.
(3) Ray, D.; Feller, D.; More, M. B.; Glendening, E. D.; Armentrout, P. B. *J. Phys. Chem.* **1996**, *100*, 1605.
(4) Ray, D.; Feller, D.; More, M. B.; Glendening, E. D.; Armentrout, P. B. *J. Phys. Chem.* **1996**, *100*, 16116.
(5) More, M. B.; Ray, D.; Armentrout, P. B. *J. Phys. Chem.* **1997**, *101*, 831.
(6) More, M. B.; Ray, D.; Armentrout, P. B. *J. Phys. Chem. A* **1997**, *101*, 4254.
(7) More, M. B.; Ray, D.; Armentrout, P. B. *J. Phys. Chem.* **1997**, *101*, 7007.
(8) Dalleska, N. F.; Tjelta, B. L.; Armentrout P. B. *J. Phys. Chem.* **1994**, *98*, 4191.
(9) Dalleska, N. F.; Honma, K.; Sunderlin, L. S.; Armentrout, P. B. *J. Am. Chem. Soc.* **1994**, *116*, 3519.
(10) Koizumi, H.; Zhang, X. G.; Armentrout, P. B. *J. Phys. Chem. A* **2001**, *105*, 2444.
(11) Koizumi, H.; Larsen, M.; Armentrout, P. B. Work in progress.
(12) Holland P. M.; Castleman A. W. *J. Am. Chem. Soc.* **1982**, *76*, 4195.
(13) Koizumi, H.; Armentrout, P. B. W. *J. Am. Soc. Mass Spectrom.* **2001**, *12*, 480.
(14) Feller, D.; Glendening, E. D.; Kendall, R. A.; Peterson, K. A. *J. Chem. Phys.* **1994**, *100*, 4981.
(15) Glendening, E. D.; Feller, D. *J. Phys. Chem.* **1995**, *99*, 3060.
(16) Feller, D.; Glendening, E. D.; Woon, D. E.; Feyereisen, M. W. *J. Chem. Phys.* **1995**, *103*, 3526.
(17) Feller, D. *J. Phys. Chem. A* **1997**, *101*, 2723.
(18) Glendening, E. D.; Feller, D. *J. Phys. Chem.* **1996**, *100*, 4790.
(19) Feller, D.; Dixon, D. A. *J. Phys. Chem. A* **2002**, *106*, 5136.
(20) Feller, D.; Glendening, E. D.; de Jong, W. A. *J. Chem. Phys.* **1999**, *110*, 1475.
(21) Feller, D.; Peterson, K. A. *J. Chem. Phys.* **1998**, *108*, 154.
(22) Feller, D.; Peterson, K. A. *J. Chem. Phys.* **1999**, *110*, 8384.
(23) Feller, D.; Dixon, D. A. *J. Phys. Chem. A* **1999**, *103*, 6413.
(24) Feller, D. *J. Chem. Phys.* **1999**, *111*, 4373.
(25) Feller, D.; Dixon, D. A. *J. Phys. Chem. A* **2000**, *104*, 3048.
(26) Feller, D.; Sordo, J. A. *J. Chem. Phys.* **2000**, *113*, 485.
(27) Feller, D.; Franz, J. A. *J. Phys. Chem. A* **2000**, *104*, 9017.
(28) Feller, D.; Dixon, D. A. *J. Chem. Phys.* **2001**, *115*, 3484.
(29) Dixon, D. A.; Feller, D. *J. Phys. Chem. A* **1998**, *102*, 8209.
(30) Dixon, D. A.; Feller, D.; Sandrone, G. *J. Phys. Chem. A* **1999**, *103*, 4744.
(31) Ruscic, B.; Feller, D.; Dixon, D. A.; Peterson, K. A.; Harding, L. B.; Asher, R. L.; Wagner, A. F. *J. Phys. Chem. A* **2001**, *105*, 1.
(32) Ruscic, B.; Wagner, A. F.; Harding, L. B.; Asher, R. L.; Feller, D.; Dixon, D. A.; Peterson, K. A.; Song, Y.; Qian, X.; Ng, C.; Liu, J.; Chen, W.; Schwenke, D. W. *J. Phys. Chem. A* **2001**, *106*, 2727.
(33) Ervin, K. M.; Armentrout, P. B. *J. Chem. Phys.* **1985**, *83*, 166.
(34) Schultz, R. H.; Armentrout, P. B. *Int. J. Mass Spectrom. Ion Processes* **1991**, *107*, 29.
(35) Muntean, F.; Armentrout, P. B. *J. Chem. Phys.* **2001**, *115*, 1213.
(36) Schultz, R. H.; Armentrout, P. B. *J. Chem. Phys.* **1992**, *96*, 1046.
(37) Schultz, R. H.; Crellin, K. C.; Armentrout, P. B. *J. Am. Chem. Soc.* **1991**, *113*, 8590.

(38) Khan, F. A.; Clemmer, D. C.; Schultz, R. H.; Armentrout, P. B. *J. Phys. Chem.* **1993**, *97*, 7978.
(39) Mark, S.; Gerlich, D. *J. Chem. Phys.* **1996**, *209*, 235.
(40) Aristov, N.; Armentrout, P. B. *J. Phys. Chem.* **1986**, *90*, 5135.
(41) Dunning, T. H., Jr. *J. Chem. Phys.* **1989**, *90*, 1007.
(42) Kendall, R. A.; Dunning, T. H., Jr.; Harrison, R. J. *J. Chem. Phys.* **1992**, *96*, 6796.
(43) Andrae, D.; Haeussermann, U.; Dolg, M.; Stoll, H.; Preuss, H. *Theor. Chim. Acta* **1990**, *77*, 123.
(44) Hehre, W. J.; Ditchfield, R.; Pople, J. A. *J. Chem. Phys.* **1972**, *56*, 2257.
(45) Hariharan, P. C.; Pople, J. A. *Theor. Chim. Acta* **1973**, *28*, 213.
(46) Clark, T.; Chandrasekhar, J.; Spitznagel, G. W.; Schleyer, P. v. R. *J. Comput. Chem.* **1983**, *4*, 294.
(47) Woon, D. E.; Dunning, T. H., Jr. *J. Chem. Phys.* **1995**, *103*, 4572.
(48) Frisch, M. J.; Trucks, G. W.; Schlegel, H. B.; Scuseria, G. E.; Robb, M. A.; Cheeseman, J. R.; Zakrzewski, V. G.; Montgomery, J. A., Jr.; Stratmann, R. E.; Burant, J. C.; Dapprich, S.; Millam, J. M.; Daniels, A. D.; Kudin, K. N.; Strain, M. C.; Farkas, O.; Tomasi, J.; Barone, V.; Cossi, M.; Cammi, R.; Mennucci, B.; Pomelli, C.; Adamo, C.; Clifford, S.; Ochterski, J.; Petersson, G. A.; Ayala, P. Y.; Cui, Q.; Morokuma, K.; Malick, D. K.; Rabuck, A. D.; Raghavachari, K.; Foresman, J. B.; Cioslowski, J.; Ortiz, J. V.; Stefanov, B. B.; Liu, G.; Liashenko, A.; Piskorz, P.; Komaromi, I.; Gomperts, R.; Martin, R. L.; Fox, D. J.; Keith, T.; Al-Laham, M. A.; Peng, C. Y.; Nanayakkara, A.; Gonzalez, C.; Challacombe, M.; Gill, P. M. W.; Johnson, B. G.; Chen, W.; Wong, M. W.; Andres, J. L.; Head-Gordon, M.; Replogle, E. S.; Pople, J. A. *Gaussian 98*, revision A.7; Gaussian, Inc.: Pittsburgh, PA, 1998.
(49) Werner, H.-J.; Knowles, P. J.; Amos, R. D.; Bernhardsson, A.; Berning, A.; Celani, P.; Cooper, D. L.; Deegan, M. J. O.; Dobbyn, A. J.; Eckert, F.; Hampel, C.; Hetzer, G.; Korona, T.; Lindh, R.; Lloyd, A. W.; McNicholas, S. J.; Manby, F. R.; Meyer, W.; Mura, M. E.; Nicklass, A.; Palmieri, P.; Pitzer, R. M.; Rauhut, G.; Schütz, M.; Stoll, H.; Stone, A. J.; Tarroni, R.; Thorsteinsson, T. MOLPRO-2000, a package of initio programs; Universität Stüttgart, Stüttgart, Germany, University of Birmingham, Birmingham, U.K., 2000.
(50) Anchell, J.; Apra, E.; Bernholdt, D.; Borowski, P.; Bylaska, E.; Clark, T.; Clerc, D.; Dachsel, H.; de Jong, B.; Deegan, M.; Dupuis, M.; Dyall, K.; Elwood, D.; Fann, G.; Fruchtl, H.; Glendening, E. D.; Gutowski, M.; Harrison, R.; Hess, A.; Jaffe, J.; Johnson, B.; Ju, J.; Kendall, R.; Kobayashi, R.; Kutteh, R.; Lin, Z.; Littlefield, R.; Long, X.; Meng, B.; Nichols, J.; Nieplocha, J.; Rendall, A.; Rosing, M.; Sandrone, G.; Stave, M.; Straatsma, T.; Taylor, H.; Thomas, G.; van Lenthe, J.; Windus, T.; Wolinski, K.; Wong, A.; Zhang, Z. NWChem, 1999.
(51) Beyer, T. S.; Swinehart, D. F. *Comm. Assoc. Comput. Machines* **1973**, *16*, 379. Stein S. E.; Rabinovitch, B. S. *J. Chem. Phys.* **1973**, *58*, 2438. Stein, S. E.; Rabinovitch, B. S. *Chem. Phys. Lett.* **1977**, *49*, 183.
(52) Gilbert, R. G.; Smith, S. C. *Theory of Unimolecular and Recombination Reactions*; Blackwell Scientific Publications: Oxford, U.K., 1990.
(53) Hales, D. A.; Lian, L.; Armentrout, P. B. *Int. J. Mass Spectrom. Ion Processes* **1990**, *102*, 269.
(54) Marcus, R. A.; Rice, O. K. *J. Phys. Colloid Chem.* **1951**, *55*, 894; Marcus, R. A. *J. Chem. Phys.* **1952**, *20*, 359. Rosenstock, H. M.; Wallenstein, M. B.; Wahrhaftig, A. L.; Eyring, H. *Proc. Natl. Acad. Sci. U.S.A.* **1952**, *38*, 667.
(55) Rodgers, M. T.; Ervin, K. M.; Armentrout, P. B. *J. Chem. Phys.* **1997**, *106*, 4499.
(56) Waage, E. V.; Rabinovitch, B. S. *Chem. Rev.* **1970**, *70*, 377.
(57) Dalleska, N. F.; Honma, K.; Armentrout, P. B. *J. Am. Chem. Soc.* **1993**, *115*, 12125.
(58) Boo, B. H.; Armentrout, P. B. *J. Am. Chem. Soc.* **1987**, *109*, 3459. Ervin, K. M.; Armentrout, P. B. *J. Phys. Chem.* **1984**, *88*, 5454. Armentrout, P. B. In *Structure/Reactivity and Thermochemistry of Ions*; Ausloos, P., Lias, S. G., Eds.; Reidel: Dordrecht, The Netherlands, 1987; p 97.
(59) Armentrout, P. B. In *Advances in Gas-phase Ion Chemistry;* Adams N. G.; Babcock, L. M., Eds.; JAI: Greenwich, U.K., 1992; Vol. 1, p 83.
(60) Armentrout, P. B.; Simons *J. Am. Chem. Soc.* **1992**, *114*, 8627.
(61) Lifshitz, C. *Adv. Mass Spectrom.* **1989**, *11*, 113.
(62) Feyereisen, M. W.; Feller, D.; Dixon, D. A. *J. Phys. Chem.* **1996**, *100*, 2993.
(63) Boys, S. F.; Bernardi, F. *Mol. Phys.* **1970**, *19*, 553.
(64) Moore, C. E. *Atomic Energy Levels*; NSRDS-NBS35; NBS: Washinton DC, 1971.
(65) Albright, T. A.; Burdett, J. K.; Whangbo, M. H. *Orbital Interactions in Chemistry*; Wiley: New York, 1985.
(66) Rothe, E. W.; Bernstein, R. B. *J. Chem. Phys.* **1959**, *31*, 1619.
(67) Stuart, H. A. *Die Struktur des Freien Molekuls*; Springer-Verlag: Berlin, **1952**, 441.
(68) Ramaswarmy, K. L. *Proc. Indian Acad. Sci., Sect. A* **1936**, *4*, 675.